falltime (Fig. 4). The duration-bandwidth product was measured to be 0·26, allowing for both the temporal and spectral system resolution. Within experimental error, this value is in agreement with the Fourier limited duration-bandwidth product expected from theory for the observed pulse shape [7].

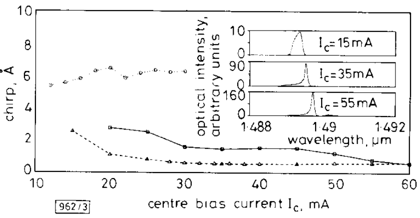

Fig. 3 *Gain switched spectral linewidth against centre contact current for two regimes of gain switching*

□ Three contact MQW DFB, $I_e = 5$ mA
△ Three contact MQW DFB, $I_e = 10$ mA
○ Single contact MQW DFB (plotted for comparison)
Inset: evolution of time averaged spectra as function of centre contact current

Control experiments have also been performed on single contact DFB lasers, with otherwise identical device structures. These generate gain switched pulses of ~30 ps width with linewidths between 6 and 8 Å, produced by identical RF drive conditions. In terms of the duration-bandwidth product however, the value exhibited by the three contact device of ~0·26 is significantly less than that of ~1·8 by the single contact devices.

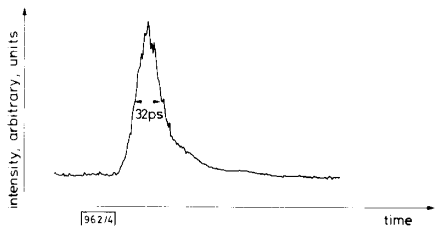

Fig. 4 *Temporal plot of gain switched optical pulse for bias current to centre contact I_c of 35 mA and with end current bias I_e of 10 mA*

Conclusions: We have demonstrated the generation of line narrowed picosecond optical pulses using a three contact DFB diode laser. Optical pulses of between 30 and 40 ps in duration, with chirp widths of ~0·6 Å have been obtained. These spectral widths are considerably reduced from between 6 and 8 Å, measured for single contact devices with otherwise identical structures and subject to the same RF drive conditions. This improvement corresponds to a reduction of duration-bandwidth product dν . *dt* from ~1·8, for equivalent single contact devices, to 0·26, obtained for asymmetric optical pulses generated by the three contact device.

Acknowledgments: The authors are grateful for financial support from the Science and Engineering Research Council (SERC), and for support from the European Community under the RACE 1027 program. They would like to thank D. Burns, Department of Physics and Astronomy, University of St Andrews for helpful discussions. Finally, P. S. Griffin would like to acknowledge both SERC and BNR Europe Ltd for personal financial support.

11th May 1992

I. H. White and P. S. Griffin* (*School of Physics, University of Bath, Claverton Down, Bath BA2 7AY, United Kingdom*)

M. J. Fice and J. E. A. Whiteaway (*BNR Europe Ltd., London Road, Harlow, Essex, CM17 9NA, United Kingdom*)

* On leave from Cambridge University Engineering Department

References

1 LIN, C., and KOCH, T. L.: 'Chirping in 1·55 µm vapour-phase-transport distributed feedback (VPTDFB) semiconductor lasers under picosecond gain switching and 4 GHz modulation', *Electron. Lett.*, 1985, **21**, pp. 958–960

2 ONODERA, N., ITO, H., and INABA, H.: 'Fourier-transform-limited single-mode picosecond optical pulse generation by a distributed feedback InGaAsP diode laser', *Appl. Phys. Lett.*, 1984, **45**, pp. 843–845

3 SUNDARESAN, H., and WICKENS, G. E.: 'Very high amplitude, minimal chirp optical pulse generation at 1·55 µm using multicontact DFBs and an erbium doped fibre amplifier', *Electron. Lett.*, 1990, **26**, pp. 725–727

4 KOBAYASHI, S., YAMADA, J., MACHIDA, S., and KIMURA, T.: 'Single mode operation of 500 Mbit/s modulated AlGaAs semiconductor laser by injection locking', *Electron. Lett.*, 1980, **16**, pp. 746–748

5 LIN, C., and MENGEL, F.: 'Reduction of frequency chirping and dynamic linewidth in high-speed directly modulated semiconductor lasers by injection locking', *Electron. Lett.*, 1984, **20**, pp. 1073–1075

6 CARTLEDGE, J. C.: 'Theoretical performance of multigigabit-persecond lightwave systems using injection locked semiconductor lasers', *J. Lightwave Technol.*, 1990, **LT-8**, pp. 1017–1022

7 DIELS, J-C. M., FONTAINE, J. J., MACMICHAEL, I. C., SIMONI, F.: 'Control and measurement of ultrashort pulse shapes (in amplitude and phase) with femtosecond accuracy', *Appl. Opt.*, 1985, **24**, pp. 1270–1283

EVEN LENGTH MEDIAN FILTERS IN OPTIMAL SIGNAL PROCESSING

J. P. Havlicek, G. R. Katz and J. C. McKeeman

Indexing terms: Filters, Signal processing

Examples are presented where the even-length median filter offers improved mean squared error characteristics over the odd-length median. This indicates that even-length filters should be considered in optimal filter design. In terms of the mean absolute error criterion, it is shown that the even-length median filter admits a representation as a generalised stack filter.

Introduction: We consider the problem of reconstructing a signal that has been corrupted by additive noise. For a signal that varies sufficiently slowly compared to the length of the filter window, this problem can be cast as one of estimating the location parameter of a single parameter distribution, where the observations are the signal samples falling within the window. The efficacy of order statistics in parameter estimation has been known for some time [1–5], and it has been shown that under appropriate assumptions the optimal order statistic filter (OSF) tends toward the median filter as the noise becomes impulsive [6]. A lesser known fact is that the statistical efficiency of the median is not necessarily monotonic in the filter length [7, 8]. Indeed, it is quite counterintuitive that the inclusion of an additional observation might be detrimental to the estimate. Typically, even-length windows are not considered in optimal filter design under the mean squared error (MSE) criterion. This is particularly true in one-dimensional signal processing, where a symmetric contiguous window of even length cannot be constructed. However, given that the behaviour of the variance of the median is nonmonotone in the presence of many types of heavily-tailed noise, we feel that even-length filters should be considered more often.

MSE criterion: We consider the simple case where the signal is constant within the filter window. For this case, minimisation of mean squared error (MSE) is equivalent to maximisation of the statistical efficiency of the estimate, and also to minimisation of the variance of the estimate. Let the inputs in the filter window be observations of N independent, identically distributed symmetric zero mean random variables $X_1, \ldots, X_N$, with density $f(x)$ and distribution $F(x)$, and let $\tilde{X}$ be the median (which is defined as the arithmetic mean of the central two order statistics when N is even). When N is odd, the variance of the median is

$$\operatorname{var}(\tilde{X}) = \frac{N!}{\frac{(N-1)}{2}!\,\frac{(N-1)}{2}!}\int_{-\infty}^{\infty} x^2[F(x)-F^2(x)]^{(N-1)/2} f(x)\,dx \quad (1)$$

For N even, the variance of $\tilde{X}$ is

$$\operatorname{var}(\tilde{X}) = \frac{N!}{4m!m!}\int_{-\infty}^{\infty}\int_{-\infty}^{x_2}(x_1+x_2)^2F^m(x_1) \times [1-F(x_2)]^m f(x_1)f(x_2)\,dx_1\,dx_2 \quad (2)$$

where $m = (N/2) - 1$.

The variance of the median of double Gaussian variables with density

$$f(x) = \frac{1}{\sqrt{(8\pi)}}[\exp(-\tfrac{1}{2}(x+b)^2) + \exp(-\tfrac{1}{2}(x-b)^2)] \quad (3)$$

is shown in Fig. 1*a* for $b = 4$. The non-monotone behaviour is striking. In this case, the mean has lower variance than either the odd or the even length medians.

Fig. 1*b* shows the variance of double lognormal variables with density

$$f(x) = \frac{1}{2(|x|-b)\sqrt{(2\pi)}}\exp(-\tfrac{1}{2}[\ln(|x|-b)-\mu]^2) \quad (4)$$

under the parameter selection $b = \mu = 2$. The variance of the mean is also shown. Finally, Fig. 1*c* shows the variances of the

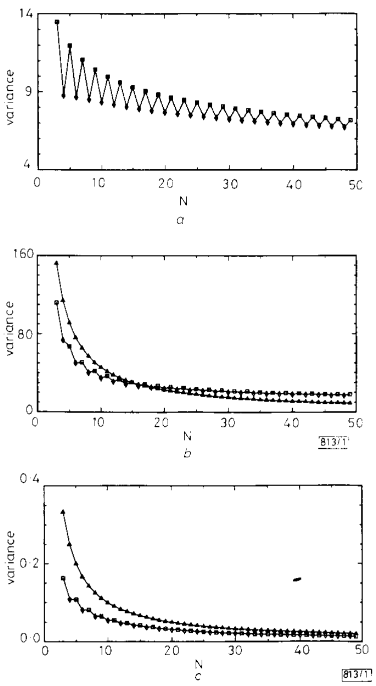

Fig. 1 *Variance of location estimators*

a Median of double Gaussian variables
b Median and mean of double lognormal variables
c Median and mean of generalised Cauchy variables
□ odd median
◇ even median
△ mean

median and mean of generalised Cauchy variables with density

$$f(x) = \frac{n\alpha^{n-1}\sin\frac{\pi}{n}}{2\pi(|x|^n + \alpha^n)} \quad (5)$$

for $n = 5$. For unity variance variables, $\alpha = \sqrt{[\sin(3\pi/n)/\sin(\pi/n)]}$. We have constructed numerous additional examples where the even length median has lower variance than the odd length median, and also has lower variance than the mean. In general, this occurs when the density displays extremely heavy tails. These results strongly suggest that even-length filters should not be ignored. A general algorithm for designing optimal MSE OSFs is available [6]. The optimisation must be carried out independently for each window length. Once the optimal filter is known for each length, the best from among these can be selected.

MAE criterion: Stack filters are an extremely large class of nonlinear operator, and an algorithm for designing minimum mean absolute error (MAE) generalised stack filters has been published recently [9]. Although the even-length median filter does not admit a stack filter representation, it turns out that any even length OSF with rational terminating coefficients can be represented as a generalised stack filter. The significance of this fact is that the technique of optimal generalised stack filter design will automatically yield the minimum MAE filter, irrespective of whether the filter length is odd or even.

To demonstrate the representation of even length OSFs as generalised stack filters, we give the stack filtering equations for the four-point median filter with input word length two bits. Let the inputs in the filter window be X^0, X^1, X^2, X^3, and let the order statistics obtained by sorting these inputs be $X^{(3)} \geq X^{(2)} \geq X^{(1)} \geq X^{(0)}$. The four-point median is defined by $\tilde{X} = \frac{1}{2}(X^{(2)} + X^{(3)})$. We use subscripts to denote binary threshold signals, and the binary threshold input signal X_k^n is defined by

$$X_k^n = \begin{cases} 1 & X^n \geq k \\ 0 & \text{otherwise} \end{cases} \quad (6)$$

The binary threshold order statistic signal $X_k^{(n)}$ is similarly defined.

In the following, all filter outputs are scaled by a factor of two, and hence take integer values in the range [0, 6]. The actual unscaled values can be obtained by shifting the binary point one position to the left in the final representation. It can be easily verified that the stack filtering equations for the binary threshold representations of (twice) $X^{(3)}$ and (twice) $X^{(2)}$ are

$$\begin{aligned} X_{2k}^{(3)} &= X_{2k-1}^{(3)} \\ &= X_k^0X_k^1 + X_k^0X_k^2 + X_k^0X_k^3 \\ &\quad + X_k^1X_k^2 + X_k^1X_k^3 + X_k^2X_k^3 \end{aligned} \quad (7)$$

and

$$\begin{aligned} X_{2k}^{(2)} &= X_{2k-1}^{(2)} \\ &= X_k^0X_k^1X_k^2 + X_k^0X_k^1X_k^3 \\ &\quad + X_k^0X_k^2X_k^3 + X_k^1X_k^2X_k^3 \end{aligned} \quad (8)$$

respectively. On constructing truth tables for the four-point median binary threshold signals in terms of the binary threshold order statistic signals, it follows that the generalised stack filtering equations for (twice) the four-point median are

$$\tilde{X}_6 = X_6^{(2)} \quad (9)$$

$$\tilde{X}_5 = X_6^{(3)}X_4^{(2)} \quad (10)$$

$$\tilde{X}_4 = X_6^{(3)}X_2^{(2)} + X_4^{(2)} \quad (11)$$

$$\tilde{X}_3 = X_6^{(3)} + X_4^{(3)}X_2^{(2)} \quad (12)$$

$$\tilde{X}_2 = X_4^{(3)} + X_2^{(2)} \quad (13)$$

and

$$\tilde{X}_1 = X_2^{(3)} \qquad (14)$$

Explicit formulation of the four-point median generalised stack filter in terms of the binary threshold input signals is obtained by substituting eqns. 7 and 8 into eqns. 9–14, and is too lengthy for this presentation. The architecture of the generalised stack filter is shown in Fig. 2.

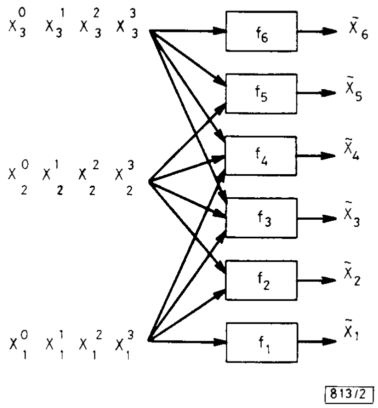

Fig. 2 *Generalised stack filter architecture for four-point median filter*

22nd April 1992

J. P. Havlicek (*Department of Electrical & Computer Engineering, The University of Texas at Austin, Austin, Texas 78712-1084, USA*)

G. R. Katz (*Naval Research Laboratory, Code 6552, Washington, DC 20375-5000, USA*)

J. C. McKeeman (*IBM Federal Sector Division, 9500 Godwin Drive, Manassas, VA 22110, USA*)

References

1 LLOYD, E. H.: 'Least-squares estimation of location and scale parameters using order statistics', *Biometrika*, 1952, **39**, pp. 88–95
2 SARHAN, A. E.: 'Estimation of the mean and standard deviation by order statistics', *Ann. Math. Statist.*, 1954, **25**, pp. 317–328
3 SARHAN, A. E.: 'Estimation of the mean and standard deviation by order statistics, part II', *Ann. Math. Statist.*, 1955, **26**, pp. 505–511
4 SARHAN, A. E.: 'Estimation of the mean and standard deviation by order statistics, part III', *Ann. Math. Statist.*, 1955, **26**, pp. 576–592
5 LWIN, T.: 'Optimal linear estimators of location and scale parameters using order statistics and related empirical Bayes estimation', *Scand. Actuarial J.*, 1976, pp. 79–91
6 BOVIK, A. C., HUANG, T. S., and MUNSON, D. C.: 'A generalization of median filtering using linear combinations of order statistics', *IEEE Trans.*, 1983, **ASSP-31**, pp. 1342–1349
7 HODGES, J. L., and LEHMANN, E. L.: 'On medians and quasi medians', *J. Am. Statist. Ass.*, 1967, **62**, pp. 926–931
8 HAVLICEK, J. P., SARKADY, K. A., KATZ, G. R., and MCKEEMAN, J. C.: 'Fast, efficient median filters with even length windows', *Electron. Lett.*, 1990, **26**, pp. 1736–1737
9 LIN, J. H., and COYLE, E. J.: 'Minimum mean absolute error estimation over the class of generalized stack filters', *IEEE. Trans.*, 1990, **ASSP-38**, pp. 663–678

GAIN ENHANCEMENT IN DISTRIBUTED ERBIUM-DOPED FIBRE AMPLIFIER BY RAMAN AMPLIFICATION OF 1480 nm PUMP RADIATION

D. M. Patrick, D. M. Spirit and D. L. Williams

Indexing terms: Optical fibres, Lasers

A 3 dB enhancement of the small-signal gain has been obtained at 1537 nm in a 12·7 km distributed erbium-doped fibre amplifier by Raman amplification of the 1480 nm pump. By copumping at 1319 nm, the 1480 nm erbium pump radiation was amplified by the $800\,cm^{-1}$ Raman gain band of silica, which resulted in an increased erbium amplifier gain at the signal wavelength of 1537 nm.

Introduction: A recent development in optical communication systems is the distributed erbium-doped silica fibre amplifier, in which low erbium ion doping concentrations are used [1, 2]. This technology offers an alternative to lumped fibre amplifiers which are typically tens of metres long. Distributed amplification may have applications in nonlinear transmission and lossless network architectures. However, the effect of background fibre loss at the 1480 nm pump wavelength places a limit on the length over which lossless transmission can be realised. Distributed erbium-doped silica fibre amplifiers have now been produced with the same background loss as that of standard telecommunications fibre. We report the use of Raman gain to reduce the effect of background fibre loss at the 1480 nm erbium pump wavelength [3]. The $800\,cm^{-1}$ Raman gain band was used to provide amplification at 1480 nm with a Raman pump wavelength of 1319 nm [4].

Experiment: Fig. 1 shows the experimental arrangement used to measure the small-signal gain enhancement in the erbium-doped fibre. A wavelength division multiplexing element 'WDM' was used to combine signals from an OTDR operating at 1537 nm and from a semiconductor pump module with a central wavelength of 1480 nm and a spectral width of 15 nm. A fused-fibre directional coupler was used to launch these signals into the erbium-doped fibre together with up to 370 mW of pump radiation from a 1319 nm CW Nd : YAG laser. The spare port of the coupler was used to monitor the launched power levels. An interference filter was used to prevent back-reflected pump light and amplified spontaneous emission affecting the performance of the OTDR. The 12·7 km erbium-doped fibre used in this experiment is singlemode and nonpolarisation maintaining. It has a background loss of 0·54 dB/km at 1319 nm, and an absorption due to the erbium doping of 1·96 dB/km at 1537 nm.

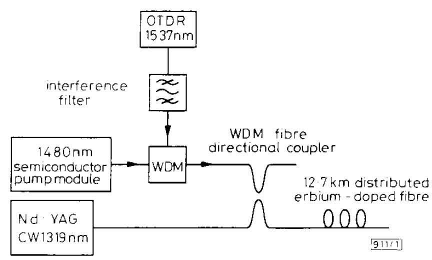

Fig. 1 *Experimental setup*

The signal level along the fibre was measured using the OTDR, and is shown in Fig. 2. In this case, 16 mW of 1480 nm pump radiation was launched into the distributed erbium-doped fibre amplifier. The lower trace represents the signal level without Raman pumping. Under these conditions, the distributed amplifier had a net loss of 1·2 dB as a result of the low 1480 nm pump power. This loss was transformed into a net small-signal gain of 2·0 dB when 370 mW of 1319 nm radiation was launched into the fibre, representing a gain enhancement of 3·2 (±0·2) dB. In this case, the 1480 nm pump power transmitted through the fibre was found to increase by 1 dB on the introduction of the Raman pump.

Fig. 3 shows the net amplifier gain as a function of 1480 nm pump power, with and without Raman amplification of the 1480 nm pump. It is thought that saturation of the 1480 nm pump transition caused the gain enhancement due to Raman amplification to decrease at higher 1480 nm pump powers.